Proceedings of the Canadian Society for Mechanical Engineering International Congress 2021
CSME Congress 2021
June 27-30, 2021, Charlottetown, PE, Canada

Performance of a Modified Drive Mechanism on a Low Temperature Differential Stirling Engine

Michael Nicol-Seto[1], David S. Nobes[1]
[1]Mechanical Engineering, University of Alberta, Edmonton, Canada
*dnobes@ualberta.ca

Abstract**—**Stirling engines are a variety of heat engines which are capable of using heat from various sources including low temperature renewables. This work examines the drive train modifications and performance results of a lab scale low temperature gamma type Stirling engine operating between a source and sink temperature of 94 °C and 5 °C respectively. The drive train was modified to use non-circular gears to dwell the engine piston motion in an effort to improve the thermodynamic work of the engine cycle. A variety of dwelling piston configurations were tested, both for the engine displacer and power pistons. Results indicate that dwelling the displacer piston reduced the engine power output by up to 27% when compared to the conventional drive mechanism, while dwelling the power piston had negligible impact on power output. Gearing the displacer piston to have shorter dwell times with slower displacement speeds did result in faster running speeds at lower engine loads, with a minor 4% improvement to maximum engine power in the best configuration.

Keywords-drive-mechanism; Stirling engine, non-circular gears, low temperature

I. INTRODUCTION

Stirling engines are a variety of thermodynamic engines that run off of external thermal sources and sinks. Their ability to use a wide variety of heat sources has spurred interest in developing Stirling engines for renewable energy recovery from sources such as solar [1], biomass [2], as well as potentially very low temperature difference heat sources such as waste heat [3] or low grade geothermal sources [4]. The useful mechanical energy available for thermodynamic conversion at low temperature ratios (below 100 °C) is inherently low, with a Carnot limit of ~25% efficiency at a source temperature of 100 °C and a sink temperature of 5 °C. For practical engines, efficiencies are much lower still [5]. As such it is desirable to maximize the thermodynamic yield of these low temperature engines by any available means. A suggested method for improving power is to better replicate the ideal thermodynamic cycle by modifying the engine drive mechanism to dwell the engine pistons [6]. This work details the construction and testing of a lab scale low temperature difference gamma Stirling engine whose drive mechanism was modified with elliptical gearing that better replicates the ideal Stirling thermodynamic cycle. Performance results of the engine are provided with recommendations as to utility of such modifications on low temperature engines.

Future Energy Systems, NSERC

II. THE STIRLING CYCLE AND PRACTICAL ENGINES

A. The ideal thermodynamic Stirling cycle

The Stirling cycle is a heat engine, where only heat flows through the engine, while the mass of the working fluid contained in the engine remains constant. The working fluid of the engine is typically a gas that undergoes discrete, sequential thermodynamic processes to form a closed loop. The idealized processes of the Stirling cycle is described below with reference to Figure 1 [7]:

1 – Isochoric heating

2 – Isothermal expansion

3 – Isochoric cooling

4 – Isothermal expansion

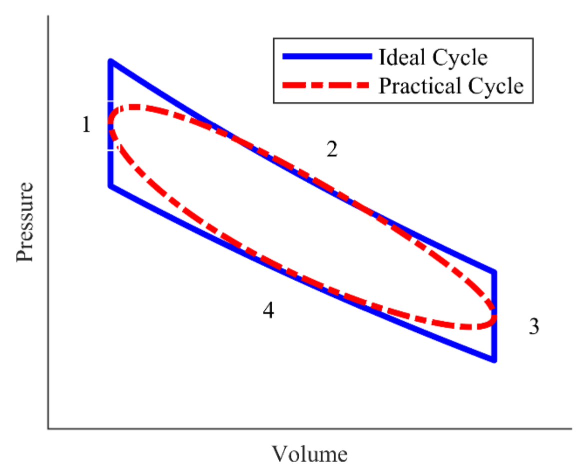

Figure 1. Representative pressure - volume diagram of the ideal and practical Stirling cycle

The indicated work done by the engine per cycle W is the difference between the absolute expansion work, W_e, minus the absolute compression work, W_c, where P is the pressure in the engine space, and V corresponds to the total engine volume [8].

$$W = W_e - W_c = \int_{V_{max}}^{V_{min}} P_e(V)dV - \int_{V_{max}}^{V_{min}} P_c(V)dV \quad (1)$$

B. *The practical kinematic Stirling engine*

Numerous variants of the Stirling cycle machine have been developed over time and are commonly classified based on the way each machine moves the engine working fluid to carry out the thermodynamic cycle [7]. This work focuses on kinematic gamma type Stirling engines [4], where kinematic indicates that the piston motions are mechanically linked and controlled via the drive mechanism. The defining characteristic of a gamma Stirling engine is that it has two piston cylinder sets as embodied in Figure 2. The isochoric heating and cooling phases are carried out by the movement of a displacer piston, which shuttles the working fluid from the expansion space of the engine to the compression space. In most large engines the gas path routs the working fluid through a set of heat exchangers and a regenerator which is the primary means of transferring heat into and out of the working space of the engine [7]. The compression and expansion phases of the cycle are accomplished via a power piston, which is driven by the differential pressure of the engine working fluid and the pressure outside of the working space, referred to as the buffer pressure [8].

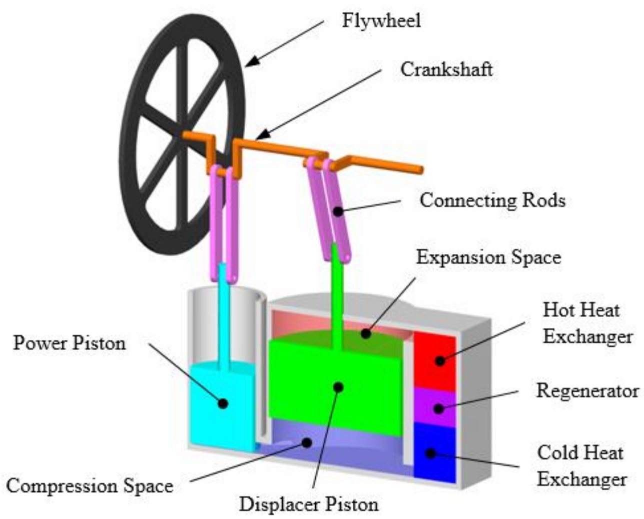

Figure 2. Generalized form of a kinematic gamma Stirling engin annotated with the primary sub-components

For most kinematic engines the pistons are linked to a common rotating output shaft via slider-crank mechanisms that convert between linear and rotational motion in an approximately sinusoidal relationship. For gamma engines the work done by the power piston drives the output shaft, while the displacer piston is driven by the same shaft, sustaining the cycle. The phasing difference between the motions of the two pistons is what causes the sequential thermodynamic processes to form the Stirling cycle. For gamma engines, a phase difference of 90° is most optimal [9]

The overlapping motions of the displacer piston and power piston result in the thermodynamic steps of the cycle overlapping as well. The thermodynamic overlap results in a practical cycle indicator diagram that is smaller and rounder than the ideal cycle as shown in Figure 1, with the associated loss of work output per cycle. If the overlap in piston motion can be reduced and the associated thermodynamic processes made more discontinuous, there is the opportunity to improve the practical engine indicator cycle to one that more closely replicates the ideal case with greater work per cycle.

C. *Cycle Modification Using Non-Circular Gearing*

Various mechanisms can be integrated into the engine drive mechanisms to achieve more discontinuous cycles with the aim of expanding the indicated work. Proposed methods have included using a cam follower drive [10], multi bar linkages [11], and elliptical gear trains [12]. This work highlights the use of oval non-circular gear pairs [13] to modify piston motion by changing the rotational speeds of the piston crank arms relative to the constant speed engine output shaft. For identical oval non-circular gear pairs the relationship between the angle of the input shaft, $\emptyset_1$, and the angle of the output shaft, $\emptyset_2$, as governed by the transmission function:

$$\tan \emptyset_2 = \frac{1+e}{1-e} \tan \emptyset_2 \quad (2)$$

where e is the elliptical eccentricity of the oval gear pair.

By phasing the lobes of the oval gears 90° to the crank arm, the dwell time of the pistons at top and bottom dead centre positions is prolonged. By phasing the gear lobes inline with the crank arms, it is also possible to shorten piston dwell time, resulting in a more linear, saw-tooth shaped piston motion profile. The prolonged or reduced dwell times alters the periods in the cycle where the piston motions and associated thermodynamic processes overlap. The modified piston motion profiles using oval gears pairs of eccentricity $e = 1/5$ and $e = 1/3$ are shown in Figure 3 against the sinusoidal motion profile.

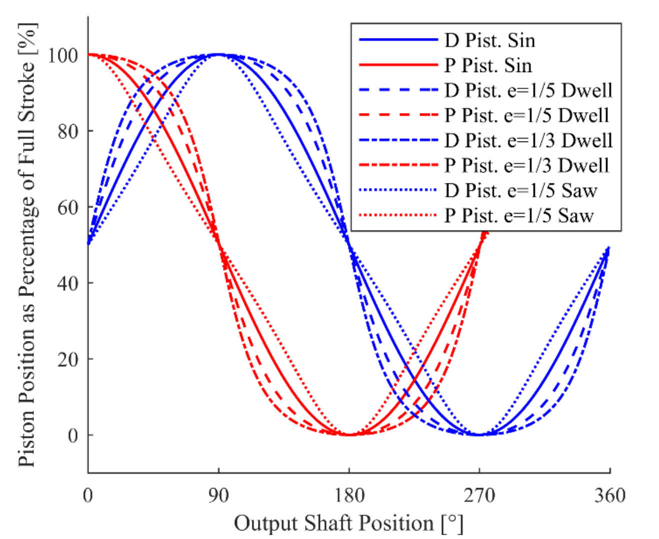

Figure 3. Normalized piston motion as a funtion of output shaft crank angle using oval gears of different eccentricity

III. THE EXPERIMENTAL GAMMA STIRLING ENGINE

A lab scale gamma Stirling engine was built in 2018 [14] to operate at low temperature differences between 0 °C and 100 °C. The engine is a kinematic gamma Stirling engine with a rotary shaft output coupled to the engine pistons via a crank-slider mechanism. Thermal energy is supplied via thermal fluid that is circulated through finned tube heat exchangers mounted in the annular gap between the displacer cylinder and the rigid pressure shell of the engine body. To reduce frictional losses of a more conventional sliding piston cylinder set, the engine uses a linearly expanding elastomer bellow as a power piston. Performance and optimization assessments of the first revision of the engine was explored in detail by Stumpf [14].

A new version of the engine's drive mechanism was made to accommodate the use of non-circular oval gearing. This updated version of the engine is shown in Figure 4. The power piston and displacer piston are coupled via crank slider mechanisms to independent crankshafts. These crankshafts are coupled to the output shaft via interchangeable gear sets. The main output shaft was upgraded with an enlarged flywheel to smooth output velocity fluctuations with added inertia to maintain a constant main shaft velocity. This was to force the piston motion to obey the desired movement profiles resulting from the functional gears. General specifications of the engine are outlined in Table I.

TABLE I. ENGINE PROPERTIES

Engine Property	Value and Units
Working Fluid	Air
Engine Minimum Volume	9.11 L
Displacer Swept Volume	5.69 L
Power Piston Swept Volume	1.78 L
Heat Exchanger Group Volume	2.25 L
Engine Dead Volume (Excluding HE Group)	1.17 L
Compression Ratio	1.2
Piston Phasing	90°

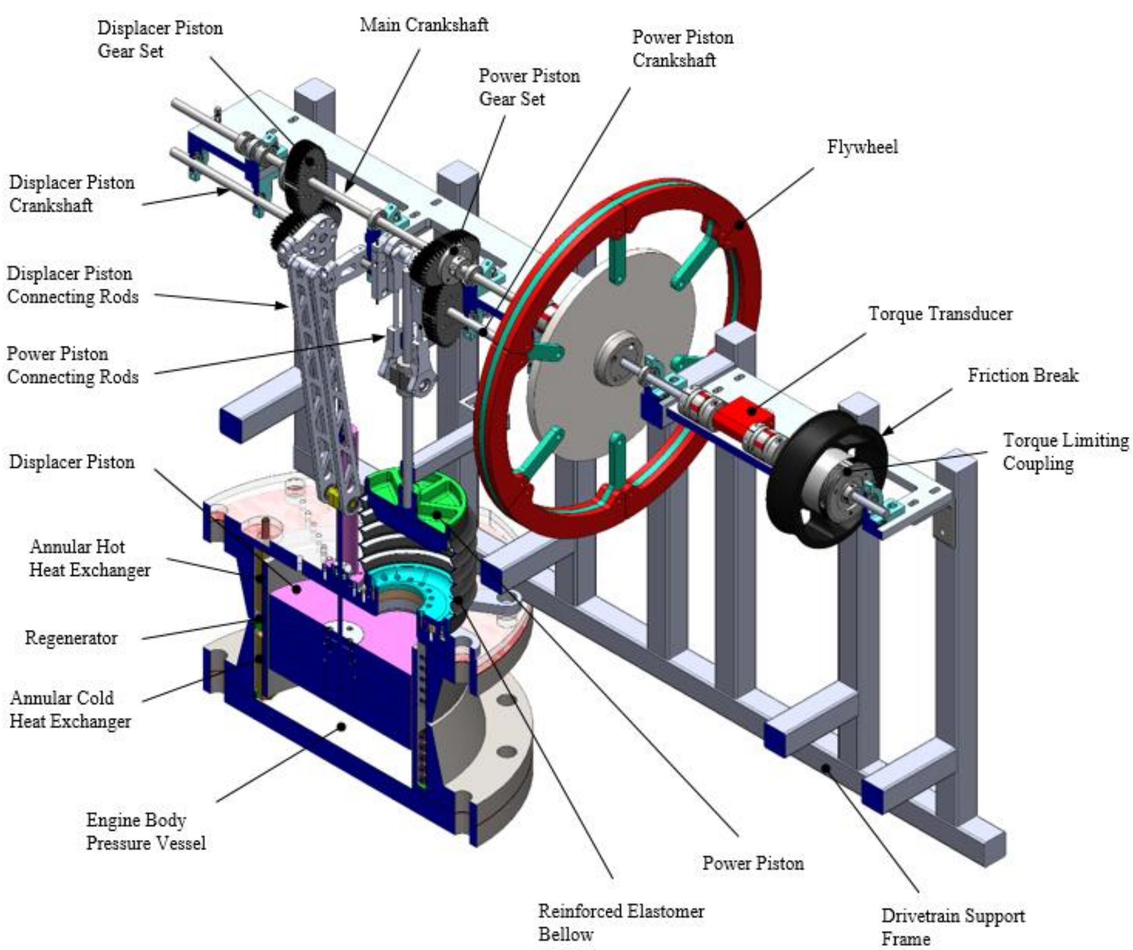

Figure 4. Partial section view of the low temperature difference gamma Stirling engine

The engine load is provided by a friction brake system that uses a weighted strap that applies friction to a drum coupled to the output shaft. Incrementally changing the weight on the strap varies the load applied to the engine allowing multiple speed and power conditions to be assessed.

IV. Testing Conditions and Configurations

The engine is coupled to an instrumented test rig that allows monitoring of engine performance parameters. The test rig instrumentation layout is shown in Figure 5. Hot thermal fluid was supplied by a hot water bath and the thermal sink was a chilled water bath. The thermal fluid is circulated by a multi-head peristaltic pump at a constant rate. The instrumentation rig directly recorded the following:

- Output shaft position
- Gauge pressure of the working fluid
- Torque output of engine
- Working fluid temperatures
- Thermal source and sink supply temperatures

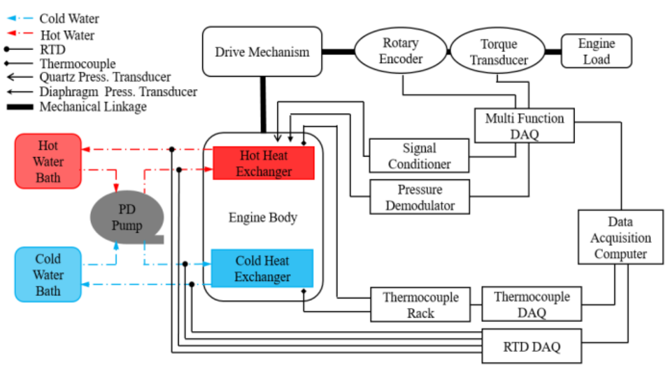

Figure 5. Engine instrumentation and data acquisition diagram

A. *Testing Conditions and Procedure*

All trial test conditions were maintained constant as much as possible between different gearing configurations. For each trial set the engine was run from unloaded free running up to stall and back down to unloaded by adding and removing fixed increments of mass to the friction break. The source and sink conditions as well as buffer pressure conditions are noted in Table II.

TABLE II. Engine Test Conditions

Engine Property	**Value and Units**
Thermal Source Fluid	Water
Source Supply Temperature (average)	94.2 ±0.4°C
Source Supply Rate	1.94 ±0.01 kg/min
Thermal Sink Fluid	Water
Sink Supply Temperature (average)	4.7 ±0.4°C
Sink Supply Rate	1.75 ±0.01 kg/min
Engine Buffer Pressure	Atmospheric

Data was collected for each load once the engine had achieved a steady state running speed. Each data set was recorded for 20s. At least two full data sets were collected for each gear configuration from unloaded to stall, back down to unloaded. Transient engine running data between loading applications was not recorded.

B. *Tested gearing configurations*

A baseline performance was established using a set of round gears with a constant 1:1 ratio. This set is equivalent to a conventional kinematic engine drive mechanism where the cranks are built into the output shaft. After the baseline was established both the power crankshaft and displacer crankshaft gear pairs were changed out in combinations. The full suite of trials is shown in Table III.

TABLE III. Tested Gearing Configurations

Trial	**Gear and Configuration Phasing**			
	Pwr. Pist. Gear Set	**Config.**	**Disp. Pist. Gear Set**	**Config**
1	$e = 0$	N/A	$e = 0$	N/A
2	$e = 0$	N/A	$e = 1/5$	Dwell
3	$e = 0$	N/A	$e = 1/5$	Saw tooth
4	$e = 1/5$	Dwell	$e = 1/5$	Saw tooth
5	$e = 1/5$	Dwell	$e = 1/5$	Dwell
6	$e = 1/5$	Dwell	$e = 0$	Dwell
7	$e = 1/3$	Dwell	$e = 0$	Dwell
8	$e = 1/3$	Dwell	$e = 1/5$	Saw tooth
9	$e = 1/3$	Dwell	$e = 1/3$	Dwell
10	$e = 0$	N/A	$e = 1/3$	Dwell
11	$e = 0$	N/A	$e = 0$	N/A

V. Results

Results presented in this work examine the maximum engine power yielded by each of the tested configurations. A summary of the results are shown in Table IV along with uncertainty $\underline{U}$. To calculate power, the average measured torque value was multiplied by the average angular speed of the output shaft.

The power curves of the various groups of configurations were plotted to examine the effects the modified motion had on the system. Only the ramping up data sets from free running to stall point for each trial group are shown.

TABLE IV. MAXIMUM RECORDED POWER PER CONFIGURATION

Trial	Measured Value			
	Speed [rpm]	U_{Speed} ± [rpm]	Power [W]	U_{Power} ± [W]
1	72.98	0.01	5.61	0.10
2	60.67	0.01	4.73	0.09
3	82.98	0.01	5.50	0.12
4	79.44	0.01	5.84	0.11
5	55.38	0.01	4.85	0.08
6	76.69	0.01	5.78	0.11
7	62.28	0.01	5.44	0.09
8	75.18	0.01	5.69	0.11
9	43.26	0.01	3.57	0.06
10	48.37	0.01	4.07	0.07
11	74.69	0.01	5.28	0.11

From Figure 6 it can be noted that dwelling the displacer piston only has broadly negative effects on engine power, with the maximum power of *e=1/3* dwelling trials producing a 27% reduction in maximum power compared to the baseline test. The most likely reason for this reduction in maximum power is the increased flow losses associated with proportionally faster displacer movement speeds caused by the dwelled cycle. It was noted by Boutammachte [10] that the acceleration and mechanical complexity of their dwelled displacer piston mechanism was not preferred over a sinusoidal system.

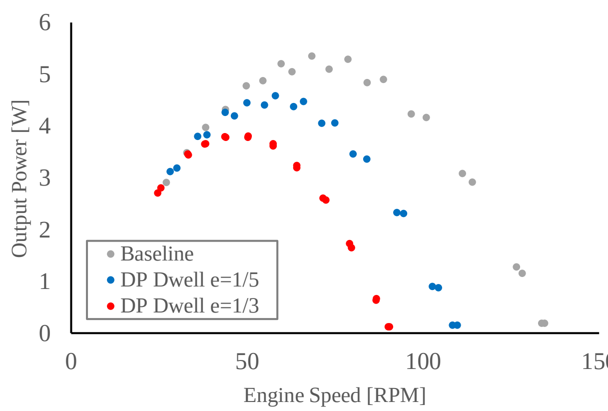

Figure 6. Engine output power curves resulting from modification of the displacer piston gearing, while maintianing conventional power piston motion

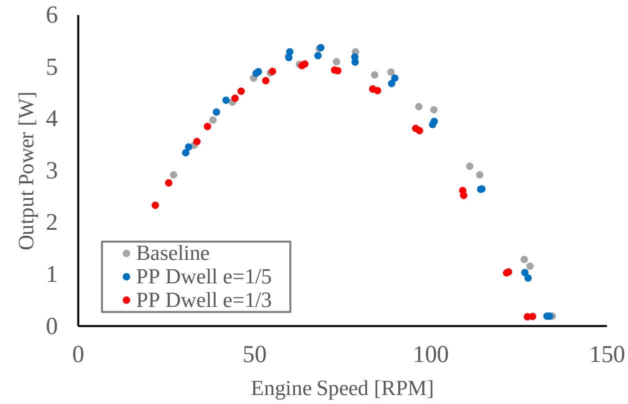

Figure 7. Engine output power curves resulting from modification of the power piston gearing while maintianing conventional displacer motion

Results of experiments involving modifying just the power piston motion are shown in Figure 7. These revealed that there was little benefit to only dwelling the power piston. The *e=1/5* trial saw a marginal 3% improvement to maximum power, while the *e=1/5* test saw a 3% decrease. Both changes were only slightly above the ±1.7% average uncertainty of the recorded results.

The saw tooth motion profiles, with slower peak displacer velocities, showed overall improvement to engine speeds. This can be seen when examining the unloaded speeds when examining Figure 8. The maximum observed power produced by the engine occurred in trial 4 with *e=1/5* dwelled power piston and a saw-tooth motion displacer piston. The maximum power of 5.54W ± 0.11W was only a 4% improvement over the maximum observed under the conventional sinusoidal set up.

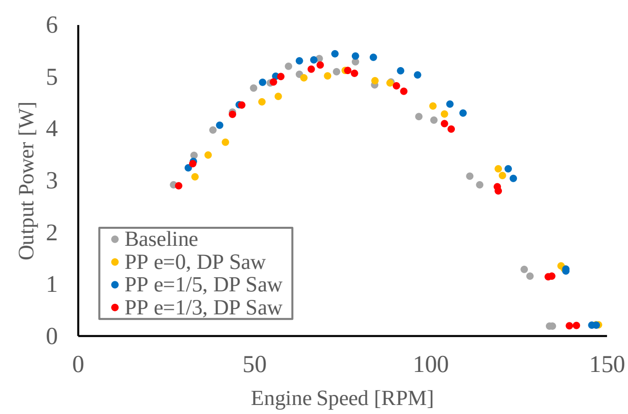

Figure 8. Engine output power curves resulting from modification of the power piston gearing while moving the displacer in a saw-tooth motion

VI. CONCLUSION

A low temperature difference gamma type Stirling engine was built and modified to examine using non-circular oval gears to improve the thermodynamic performance and power output of the engine. Testing revealed that dwelling the piston motion to achieve a more discrete thermodynamic process to better emulate the ideal cycle had either a negligible effects, as was the case for dwelling the power piston, or substantially reduced the maximum power output, as was the case for the dwelled displacer piston.

It was found that moving the displacer in a saw-tooth pattern with more constant, slower velocities had either minor or negligible improvements to maximum power output, but resulted in faster running speeds under low load conditions. Overall the results indicate that deviating from the conventional, overlapping sinusoidal piston motion is likely not worth the added mechanical complexity of the system under the tested conditions. Further investigation will examine the gearing effect on the engine pressure-volume indicator diagrams and any relationships between the mechanism and other engine performance parameters such as engine efficiency.

ACKNOWLEDGMENT

The authors acknowledge financial support from Future Energy Systems (FES) and the Natural Sciences and Engineering Research Council (NSERC) of Canada.

REFERENCES

[1] B. Kongtragool and S. Wongwises, “A review of solar-powered Stirling engines and low temperature differential Stirling engines,” *Renew. Sustain. Energy Rev.*, vol. 7, no. 2, pp. 131–154, 2003.

[2] ÖkoFEN Heiztechnik GmbH, “Pellematic Condens_e”, oekofen.com. https://www.oekofen.com/de-de/pellematic-condens_e/ (accessed Feb. 11, 2021)

[3] K. Wang, S. R. Sanders, S. Dubey, F. H. Choo, and F. Duan, “Stirling cycle engines for recovering low and moderate temperature heat: A review,” *Renew. Sustain. Energy Rev.*, vol. 62, no. September, pp. 89–108, 2016.

[4] J. Egas and D. M. Clucas, “Stirling Engine Configuration Selection,” *Energies*, pp. 1–22, 2018.

[5] A. Organ, “An Ideal Thermodynamic Reference Cycle,” in *Thermodynamics and Gas Dynamics of the Stirling Cycle Machine*, New York, USA, Cambridge, 1992

[6] I. Kolin, “Flat Plate and Discontinous Motion”, in *Stirling Motor History – Theory – Practice*, Zagreb, S.F.R Yugoslavia, Zagreb University Publications Ltd, 1991

[7] I. Urieli and D. M. Berchowitz, “Introduction,” in *Stirling Cycle Engine Analysis*, Bristol, England, Adam Hilger Ltd, 1984

[8] J. Senft, “Energy Transfer In Cyclic Heat Engines,” in *Mechanical Efficiency of Heat Engines*, New York, USA, Cambridge, 2007

[9] J. Senft “Optimum Stirling Engine Geometry”, *Int. J. of Energy Res*, vol. 26, pp. 1087–1101, 2002

[10] N. Boutammachte and J Knorr, “Field-test of a solar low delta-T Sirling engine”, *Solar Energy*, vol 86, pp.1849-1856, Apr. 2012.

[11] S. Kota, “Generic Models for Designing Dwell Mechanisms: A Novel Kinematic Design for Stirling Engines as an Example”, *Journal of Mechanical Design*, vol. 113, pp. 446-450, Dec 1991

[12] H.W. Fang, K.E. Herold, H.M. Holland, and E.H. Beach, "A novel Stirling engine with an elliptic drive," *IECEC 96. Proceedings of the 31st Intersociety Energy Conversion Engineering Conference*, Washington, DC, USA, 1996, pp. 1232-1237

[13] F. Litvin, “Elliptical Gears and Gear Drives,” in *Noncicular Gears: Deasign and Generation,* New York, USA, Cambridge, 2009

[14] C. Stumpf, “Parameter Optimization of a Low Temperature Difference Gamma-Type Stirling Engine to Maximize Shaft Power”, M.S. thesis, Mech. Eng. Dept., Univ. of Alberta, Edmonton, Canada, 2019